Mode of Binding of Methyl Acceptor Substrates to the Adrenaline-Synthesizing Enzyme Phenylethanolamine *N*-Methyltransferase: Implications for Catalysis†

Christine L. Gee,‡ Joel D. A. Tyndall,§ Gary L. Grunewald,|| Qian Wu,⊥ Michael J. McLeish,⊥ and Jennifer L. Martin*,‡

Institute for Molecular Bioscience and ARC Special Research Centre for Functional and Applied Genomics, University of Queensland, Brisbane, Queensland, 4072 Australia, National School of Pharmacy, University of Otago, P.O. Box 913, Dunedin, New Zealand 9015, Department of Medicinal Chemistry, The University of Kansas, Lawrence, Kansas 66045-7582, and College of Pharmacy, University of Michigan, Ann Arbor, Michigan 48109

Received August 16, 2005; Revised Manuscript Received October 24, 2005

ABSTRACT: Here we report three crystal structure complexes of human phenylethanolamine *N*-methyltransferase (PNMT), one bound with a substrate that incorporates a flexible ethanolamine side chain (*p*-octopamine), a second bound with a semirigid analogue substrate [*cis*-(1*R*,2*S*)-2-amino-1-tetralol, *cis*-(1*R*,2*S*)-AT], and a third with *trans*-(1*S*,2*S*)-2-amino-1-tetralol [*trans*-(1*S*,2*S*)-AT] that acts as an inhibitor of PNMT rather than a substrate. A water-mediated interaction between the critical β-hydroxyl of the flexible ethanolamine group of *p*-octopamine and an acidic residue, Asp267, is likely to play a key role in positioning the side chain correctly for methylation to occur at the amine. A second interaction with Glu219 may play a lesser role. Catalysis likely occurs via deprotonation of the amine through the action of Glu185; mutation of this residue significantly reduced the k_{cat} without affecting the K_m. The mode of binding of *cis*-(1*R*,2*S*)-AT supports the notion that this substrate is a conformationally restrained analogue of flexible PNMT substrates, in that it forms interactions with the enzyme similar to those observed for *p*-octopamine. By contrast, *trans*-(1*S*,2*S*)-AT, an inhibitor rather than a substrate, binds in an orientation that is flipped by 180° compared with *cis*-(1*R*,2*S*)-AT. A consequence of this flipped binding mode is that the interactions between the hydroxyl and Asp267 and Glu219 are lost. However, the amines of inhibitor *trans*-(1*S*,2*S*)-AT and substrate *cis*-(1*R*,2*S*)-AT are both within methyl transfer distance of the cofactor. These results suggest that PNMT catalyzes transfer of methyl to ligand amines only when "anchor" interactions, such as those identified for the β-hydroxyls of *p*-octopamine and *cis*-AT, are present.

The final step in the biosynthesis of epinephrine (adrenaline) from norepinephrine (noradrenaline) involves the methylation of the primary amine in a reaction catalyzed by the enzyme phenylethanolamine *N*-methyltransferase (PNMT,[1] EC 2.1.1.28, Figure 1A). PNMT is an ~31 kDa protein expressed in the adrenal medulla and in selected neurons in the central nervous system (*1*). Although the physiological substrate of PNMT is the *R* enantiomer of norepinephrine (Figure 1), phenylethanolamine (PEA) is used as a substrate in kinetic analyses because norepinephrine autoxidizes to form noradrenochrome (*2*).

Hydroxyphenylethanolamines (e.g., *p*-octopamine, *o*-octopamine, normetanephrine, and norparanephrine) and halogen-substituted phenylethanolamines (e.g., 2-chloro, 3,4-dichloro, 3-fluoro, 4-fluoro, 3-bromo, and 4-bromo) are also substrates of PNMT (*3*−*6*). However, compounds that lack a β-hydroxyl such as phenylethylamines and amphetamines are not substrates and instead inhibit PNMT (*4*, *7*). Semirigid and rigid analogues of phenylethanolamine have been developed for the further investigation of the structure−activity and binding mode of PNMT substrates and inhibitors (*8*−*13*). A significant finding from this early work was that only one of the *cis*-(1*R*,2*S*) and *trans*-(1*S*,2*S*) isomers of the semirigid PEA analogue 2-amino-1-tetralol (AT) (Figure 1B) is utilized for catalysis by PNMT; the *cis*-(1*R*,2*S*) isomer is a substrate, whereas the *trans*-(1*S*,2*S*) isomer is an inhibitor of the enzyme (*9*).

Structure−activity studies have led to a number of findings regarding PNMT substrate requirements. (1) Stereochemistry may be important; for example, the hydroxyl of the semirigid analogue tetralol must be *R* rather than *S* for substrate activity (*9*). (2) A fully extended side chain conformation for flexible substrates is optimal for binding (*14*). (3) The bound conformation of flexible substrates is likely to have the amine coplanar with the aromatic ring (*15*).

† This work was supported by an Australian Research Council grant to J.L.M. and J.D.A.T. and National Institutes of Health Grant HL34193 to G.L.G.

* To whom correspondence should be addressed. Phone: +61 7 3346 2016. Fax: +61 7 3346 2101. E-mail: j.martin@imb.uq.edu.au.

‡ University of Queensland.

§ University of Otago.

|| The University of Kansas.

⊥ University of Michigan.

[1] Abbreviations: PNMT, phenylethanolamine *N*-methyltransferase; hPNMT, human PNMT; *wt*, wild type; $hPNMT_A$, molecule A in the asymmetric unit of hPNMT crystals; $hPNMT_B$, molecule B in the asymmetric unit of hPNMT crystals; PEA, phenylethanolamine; AT, 2-amino-1-tetralol; AdoMet, *S*-adenosyl-L-methionine; AdoHcy, *S*-adenosyl-L-homocysteine; THIQ, 1,2,3,4-tetrahydroisoquinoline; GNMT, glycine *N*-methyltransferase; GAMT, guanidinoacetate *N*-methyltransferase; CNS, Crystallography and NMR System; PEG 6K, polyethylene glycol with an average molecular mass of 6 kDa; C_E, ϵ-carbon of AdoMet; S_D, δ-sulfur of AdoMet or AdoHcy; SEM, standard error of the mean.

10.1021/bi051636b CCC: $30.25
Published on Web 12/01/2005

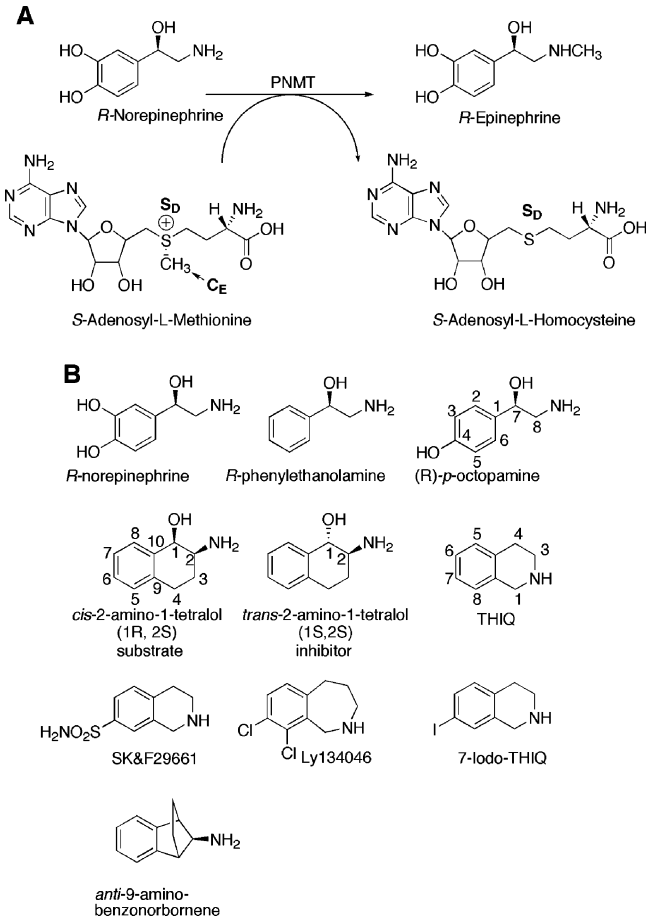

FIGURE 1: Catalytic reaction and chemical structures. (A) Physiological reaction catalyzed by PNMT that converts (*R*)-norepinephrine to (*R*)-epinephrine. (B) Substrates and inhibitors of PNMT mentioned in the text and numbering schemes for (*R*)-*p*-octopamine and the 2-amino-1-tetralols used in Table 3.

In our previous work, we have determined several crystal structures of human PNMT (hPNMT) complexed with AdoHcy and different semirigid analogue inhibitors based on the 1,2,3,4-tetrahydroisoquinoline moiety (THIQ, Figure 1B) (*16*, *17*). The observed mode of binding of THIQ inhibitors in the crystal structures allowed the development of a model for norepinephrine substrate binding (*16*). This model supported previous structure−activity studies (*18*) that proposed that the THIQ amine mimics the β-hydroxy rather than the amine of the β-hydroxyethanolamine of PEA and norepinephrine substrates (*16*). The model of norepinephrine identified Asp267 as a potential interaction partner of the β-hydroxyl group of substrates such as PEA and norepinephrine. Mutagenesis of Asp267 (D267A) supported this hypothesis, in that substrates with a flexible ethanolamine side chain had a lower k_{cat} value for this variant than the *wt* enzyme (*19*), whereas the value of k_{cat} for the rigid analogue substrate *anti*-9-amino-6-(trifluoromethyl)benzonorbornene, which lacks a β-hydroxyl, was essentially unchanged. This result suggested that the role of Asp267 is to position the flexible portion of norepinephrine or PEA within the active site (*19*). Other residues implicated in binding to norepinephrine on the basis of this model were Glu219 and Lys57.

Here we present crystal structures of hPNMT complexed with methyl acceptor substrates and cofactor products, allowing identification of the residues and interactions involved in substrate binding and revealing for the first time the binding mode of hPNMT substrates. The structures also allow a preliminary analysis, supported by mutagenic studies, of the catalytic mechanism of the enzyme. In addition, the pair of structures of hPNMT complexed with AdoHcy and either *cis*-(1*R*,2*S*)-AT or *trans*-(1*S*,2*S*)-AT shows that a similar molecular scaffold does not necessarily translate to a similar binding mode, and helps to explain why one is a substrate for the methyl transfer reaction catalyzed by the enzyme and the other inhibits this reaction.

MATERIALS AND METHODS

Crystallization of PNMT. hPNMT with a C-terminal His_6 tag was expressed and purified as described previously (*20*, *21*). The protein was concentrated to 50−60 mg/mL and mixed with substrate or inhibitor (final concentration of 50 mM) and cofactor product *S*-adenosyl-L-homocysteine (AdoHcy, final concentration of 1.7 mM), bringing the final concentration of protein to 33−40 mg/mL or 1−1.2 mM. The protein mixture was crystallized by hanging drop vapor diffusion using drops of 1 μL of protein and 1 μL of precipitant over 100 μL of precipitant [5−8% PEG 6K, 0.25 M LiCl, and 0.1 M sodium cacodylate (pH 5.5−6.0)].

Data Collection. Crystals of the appropriate size (~0.25 mm × 0.25 mm × 0.25 mm) were cryoprotected by being dipped into mother liquor with 25% glycerol for 30 s to 2 min and flash-cooled in a N_2 gaseous stream. X-ray diffraction data were measured using X-rays generated by a Rigaku FR-E copper rotating anode generator operating at 45 kV and 45 mA with Osmic Confocal Max-Flux optics (either HiRes^2 or Maxscreen). Reflections were measured using an R-AXIS IV^{++} imaging plate area detector. A Cryo Industries CryoCool LN2 was used for cooling the crystals during cryocrystallographic data measurement. Data were processed using Crystal Clear (Rigaku Corp.), and phasing was carried out using CNS version 1.1 (*22*).

Structure Determination. The structures were determined by difference Fourier methods using the hPNMT−AdoHcy−SK&F29661 structure [PDB entry 1HNN (*16*)] as the model. The asymmetric unit was chosen so that the disulfide bonds observed in the structure were formed between molecules in the same asymmetric unit and not between symmetry-related molecules. Model building was performed using O (*23*), and the structures were refined using CNS version 1.1 (*22*) or REFMAC (*24*) followed by a final refinement in CNS. Initial coordinates for the substrates and inhibitor were generated using the Insight II 2000.1 (Accelrys) builder module. Topology and parameter files for ligands were generated using PRODRG (*25*) or XPLO2D (*26*), and modified where necessary. The procedure used was to refine the structure of the protein against the diffraction data first, followed by addition of water molecules, then AdoHcy, and finally the substrate or inhibitor. The criteria for including a water molecule were the presence of $2F_o - F_c$ density at 1σ and $F_o - F_c$ density at 3σ and a hydrogen bond donor or acceptor within 3.8 Å. R_{free} analysis (10% of reflections) was used for cross-validation (*27*). The histidine tag engineered at the C-terminus of hPNMT to facilitate purification was not visible in the electron density. When water atoms Wat1 and Wat2 (with no density in the $2F_o - F_c$ map at 1σ, but

density at 3σ in the $F_o - F_c$ map) were modeled into the crystal structure, they were positionally refined for 10 cycles in CNS followed by individual *B*-factor refinement in CNS for 20 cycles (the *B*-factors were arbitrarily set to 40 before refinement).

AdoMet was modeled into the active site of hPNMT structures by the addition of a methyl group onto the refined structure of AdoHcy using SYBYL 7.0 with update #1 from Tripos Inc. (1699 S. Hanley Rd., St. Louis, MO).

Coordinates and structure factors for the three crystal structures have been deposited as Protein Data Bank entries 2AN3, 2AN4, and 2AN5.

Preparation of hPNMT Variants. The mutants were prepared using Pfu DNA polymerase and the QuikChange site-directed mutagenesis kit (Stratagene), using pET17PNMT-His (*20*) as the DNA template. The forward primers used for the mutagenesis are shown below with the mutated codons underlined, with the lowercase letters indicating a base change from the wild-type sequence: Y35F, 5′-TTCGAGCCaCGCGCCTtCCTCCGCAACAAC-3′; E185Q, 5′-GCCTTCTGCTTGcAaGCaGTGAGCCCAGATCTTG-3′; E185A, 5′-GCCTTCTGCTTGGcaGCaGTGAGCCCA-GATCTTG-3′; E185D, 5′-GCCTTCTGCTTGGAcGCAGT-GAGCCCAGATCTTG-3′; and E219Q, 5′-CGGGGCCC-TcGAGcaGTCGTGGTACC-3′.

In addition to creating the Y35F mutation, this primer introduced a silent mutation which resulted in the loss of a *Bss*HII restriction site. The Glu185 mutagenesis primers all introduced silent mutations leading to the gain of a *Bts*I restriction site, while the E219Q primer introduced a *Xho*I site. Following mutagenesis, the template DNA was removed by treatment with *Dpn*I and the remaining PCR products were transformed into *Escherichia coli* strain JM109 (Promega). Single colonies were picked, and in each case, their DNA was isolated and screened for the desired mutation using the appropriate restriction enzyme. The fidelity of the PCR amplification and the presence of the mutation were confirmed by sequencing. The plasmids were then transformed into *E. coli* strain BL21(DE3)pLysS (Novagen), and the mutants were expressed and purified by affinity followed by size exclusion chromatography as described previously (*20*, *21*).

Determination of Kinetic Constants. A typical assay mixture consisted of 25 μL of 0.5 M phosphate buffer (pH 8.0), 5 μL of [*methyl*-^{3}H]AdoMet containing approximately 2.5×10^5 dpm (specific activity of approximately 15 Ci/mmol), varying amounts of PEA and unlabeled AdoMet, 20 μL of enzyme, and sufficient water to achieve a final volume of 250 μL. After incubation for 30 min at 30 °C, the reaction was quenched by addition of 500 μL of 0.5 M borate buffer (pH 10.0) and the mixture was extracted with 2 mL of a toluene/isoamyl alcohol mixture (7:3). A 1 mL portion of the organic layer was removed, transferred to a scintillation vial, and diluted with cocktail for counting. PEA and AdoMet concentrations were varied between $0.3K_m$ and $3K_m$. Initial rate data were fit to the equation for a sequential reaction (*28*) using SigmaPlot 8.0 with the Enzyme Kinetics Module from Systat Software Inc. (Richmond, CA). The K_i value for *trans*-(1*S*,2*S*)-AT was determined at a fixed AdoMet concentration of 5 μM. The concentration of PEA was varied between $0.4K_m$ and $2.5K_m$, while the inhibitor concentration was varied between $0.4K_i$ and $2.5K_i$. Initial velocity data were then fitted to eq 1 again using SigmaPlot 8.0.

$$v = \frac{V_{max}[S]}{[S] + K_m(1 + [I]/K_i)} \quad (1)$$

Table 1: Kinetic Constants for hPNMT with Selected Substrates and Inhibitors[a]

substrate or inhibitor	K_m (μM)	K_i (μM)	k_{cat} (min^{-1})	k_{cat}/K_m (M^{-1} min^{-1})
(±)-PEA	99 ± 6	−	2.6 ± 0.1	2.6×10^4
(±)-octopamine	5.5 ± 0.6	−	1.2 ± 0.1	2.2×10^5
cis-(1*R*,2*S*)-AT	5.3 ± 0.8	−	0.29 ± 0.02	5.5×10^4
trans-(1*S*,2*S*)-AT	−	2.10 ± 0.03	−	−

[a] Kinetic data were obtained in 50 mM phosphate buffer (pH 8.0) at 30 °C. Each datum point is an average of at least three individual measurements. Values are reported as ±standard error of the mean (SEM).

RESULTS

Kinetic data for hPNMT and *p*-octopamine, *cis*-(1*R*,2*S*)-AT, and *trans*-(1*S*,2*S*)-AT are summarized in Table 1. These data confirm results obtained previously with bovine PNMT, that *cis*-(1*R*,2*S*)-AT is a substrate whereas *trans*-(1*S*,2*S*)-AT is an inhibitor (*9*). The K_m and K_i values indicate that all three compounds bind to hPNMT in low micromolar concentrations. High-resolution diffraction data were measured for complexes of the hPNMT−AdoHcy species with *p*-octopamine, *cis*-(1*R*,2*S*)-AT, or *trans*-(1*S*,2*S*)-AT, and the three structures were refined (Table 2). The crystal structures are isomorphous with previously published crystal structures of hPNMT, with two copies of the enzyme present in the asymmetric unit. In all three of the refined structures, the PNMT protein fold and the binding mode and contacts formed to the cofactor product AdoHcy are essentially identical to those described previously for hPNMT structures complexed with AdoHcy and semirigid analogue inhibitors (*16*, *17*). The electron density maps also revealed the presence of the expected substrate or inhibitor in the active site.

hPNMT−Substrate Structures. The crystal structures show that the substrates *p*-octopamine and *cis*-(1*R*,2*S*)-AT interact with the enzyme at the same site that binds hPNMT inhibitors. Furthermore, the aromatic rings of the substrates bind to the enzyme between the side chains of Phe182 and Asn39, in the same manner as the aromatic rings of the THIQ moieties of previously determined hPNMT−inhibitor structures (*16*, *17*).

p-Octopamine. The chemical structure of *p*-octopamine comprises an aromatic ring substituted with a flexible β-hydroxyethylamine side chain and a *p*-hydroxy group (Figure 1B). *B*-Factors of atoms in the side chain of *p*-octopamine (53−54 Å^2 in PNMT$_A$ and 45−48 Å^2 in PNMT$_B$) are similar to those observed for atoms in the phenyl ring (51−54 Å^2 in PNMT$_A$ and 42−46 Å^2 in PNMT$_B$), suggesting that the side chain conformation becomes ordered upon binding to the enzyme (by comparison, the average *B*-factor for hPNMT atoms is 47 Å^2). Previous work had identified structural and conformational preferences for substrates of PNMT, and the crystal structure validates these. First, whereas a racemic mixture of (*R*)- and (*S*)-octopamine was used for crystallization and kinetic studies, the *R*

Table 2: Statistics for Crystallographic Data Measurement and Structure Refinement

	(*R*)-*p*-octopamine with AdoHcy	*cis*-(1*R*,2*S*)-AT with AdoHcy	*trans*-(1*S*,2*S*)-AT with AdoHcy
space group	$P4_32_12$	$P4_32_12$	$P4_32_12$
unit cell			
$a = b$ (Å)	93.5	93.8	94.0
c (Å)	188.7	187.1	187.5
$\alpha = \beta = \gamma$ (deg)	90	90	90
no. of observations	299485	286033	233616
no. of unique reflections	43061	42859	29890
resolution range (Å) (top shell)	42−2.2 (2.28−2.20)	66−2.2 (2.28−2.20)	39−2.5 (2.59−2.50)
redundancy	6.95 (6.99)	6.67 (6.28)	7.82 (7.87)
$I/\sigma I$	11.9 (4.3)	12.8 (3.7)	13.9 (4.1)
completeness[a] (%)	100 (100)	99.2 (99.4)	100 (100)
R_{merge}[b] (%)	8.0 (44.7)	7.9 (46.4)	7.6 (46.2)
refinement			
no. of reflections ($\|F\| > 0$)			
total	43059	42856	29889
test set	4343	4317	2990
R_{cryst}[c]/R_{free}[d] (%)	23.0/27.4 (41.8/43.3)	21.7/25.6 (37.0/39.2)	21.7/24.6 (34.8/39.7)
no. of non-hydrogen atoms	4487	4508	4417
no. of protein non-hydrogen atoms	4154	4176	4164
no. of ligand non-hydrogen atoms	79	76	81
no. of waters	254	256	172
rmsd from ideal geometry			
bond lengths (Å)	0.007	0.006	0.007
bond angles (deg)	1.4	1.3	1.4
coordinate error			
from Luzzati plot (Å)	0.32	0.29	0.32
from cross-validated Luzzati plot (Å)	0.38	0.35	0.39
average *B*-factor (Å^2)			
all atoms	47.2	44.4	56.2
protein	47.0	44.1	56.3
substrate	44.3	40.4	50.9
cofactor	48.9	38.3	58.5
waters	49.7	49.3	55.6
Ramachandran plot (%)			
most favored region	91.1	92.2	91.8
disallowed region	0	0	0

[a] Completeness indicates the number of measured independent reflections divided by the total number of theoretical independent reflections. [b] $R_{merge} = \sum|I_{obs} - I_{av}|/\sum I_{av}$, over all symmetry-related observations. [c] $R_{cryst} = \sum|F_{obs} - F_{calc}|/\sum|F_{obs}|$, over all reflections. [d] R_{free} is calculated as for R_{cryst} from 10% of the data excluded from refinement. Values in parentheses are for the top shell of data.

enantiomer (*9*) appeared to be preferentially bound to the enzyme, as determined by the fit to the electron density [though the possibility that a small proportion of (*S*)-octopamine is bound to the enzyme cannot be ruled out]. Second, the structure of hPNMT with bound *p*-octopamine revealed that the flexible portion of the substrate adopts an extended (rather than *gauche*) conformation (*8*, *14*) (Figures 2A and 3A). Third, the amine is coplanar with the aromatic ring (*15*).

Also as predicted previously, the β-hydroxyl of the octopamine side chain occupies essentially the same position and forms similar interactions as the amine of bound THIQ inhibitors (Figure 3A and 4A) (*16*, *18*). Thus, the β-hydroxyl is within direct hydrogen bonding distance of Glu219 (2.9−3.0 Å) (Table 3 and Figure 2A). A water-mediated interaction with Asp267 is particularly strong, as indicated by the continuous $F_o - F_c$ omit electron density (4σ) linking the substrate hydroxyl, the ordered water, and the acidic side chain of Asp267 (Figure 3A). The distances to this water (Wat3, Table 3) are short (β-OH···2.5−2.6 Å···water···2.4−2.6 Å···Asp267), suggestive of a strong (low-barrier) hydrogen bond (*29*). The β-hydroxyl also forms a water-mediated interaction with the side chain of Asn39.

The *p*-hydroxyl group forms a water-mediated hydrogen bond with the side chain of Lys57 (Figure 2A), confirming the involvement of this side chain in ligand orientation (*16*, *17*). The same ordered water also mediates an interaction between the *p*-hydroxyl and the backbone oxygen of Asn39. Superimposition of the hPNMT crystal structures reveals that the *p*-hydroxyl group of the octopamine substrate occupies essentially the same position as the sulfonamide sulfur, 8-chloro, and iodo aromatic substituents of the PNMT inhibitors SK&F29661, LY134046, and 7-iodo-THIQ, respectively (Figure 4A) (*17*).

The amine of *p*-octopamine is within 3.5 Å of the aromatic ring of Tyr222, suggesting a possible amino−aromatic interaction. There are no other direct interactions between the substrate amine and the enzyme, but the crystal structure suggests two possible water-mediated interactions. Thus, in one of the two hPNMT molecules in the asymmetric unit ($hPNMT_A$), a water (Wat1) forms a hydrogen bond network between the substrate amine and the side chains of Glu185 and Glu219. In the second hPNMT molecule ($hPNMT_B$), Wat1 may be present, but at a lower occupancy; $F_o - F_c$ density is found at the 3σ contour level, but $2F_o - F_c$ density is only obvious at 0.5σ. Instead, in $hPNMT_B$, a water (Wat2) is located between the amine and the sulfur of AdoHcy, close to the position of the donor methyl group if it were AdoMet bound in the cofactor site rather than AdoHcy. Curiously, there is $F_o - F_c$ density at 3σ at the Wat2 position in $hPNMT_A$, but no $2F_o - F_c$ density is obvious, even at 0.5σ. If waters are modeled and refined at both Wat1 and Wat2

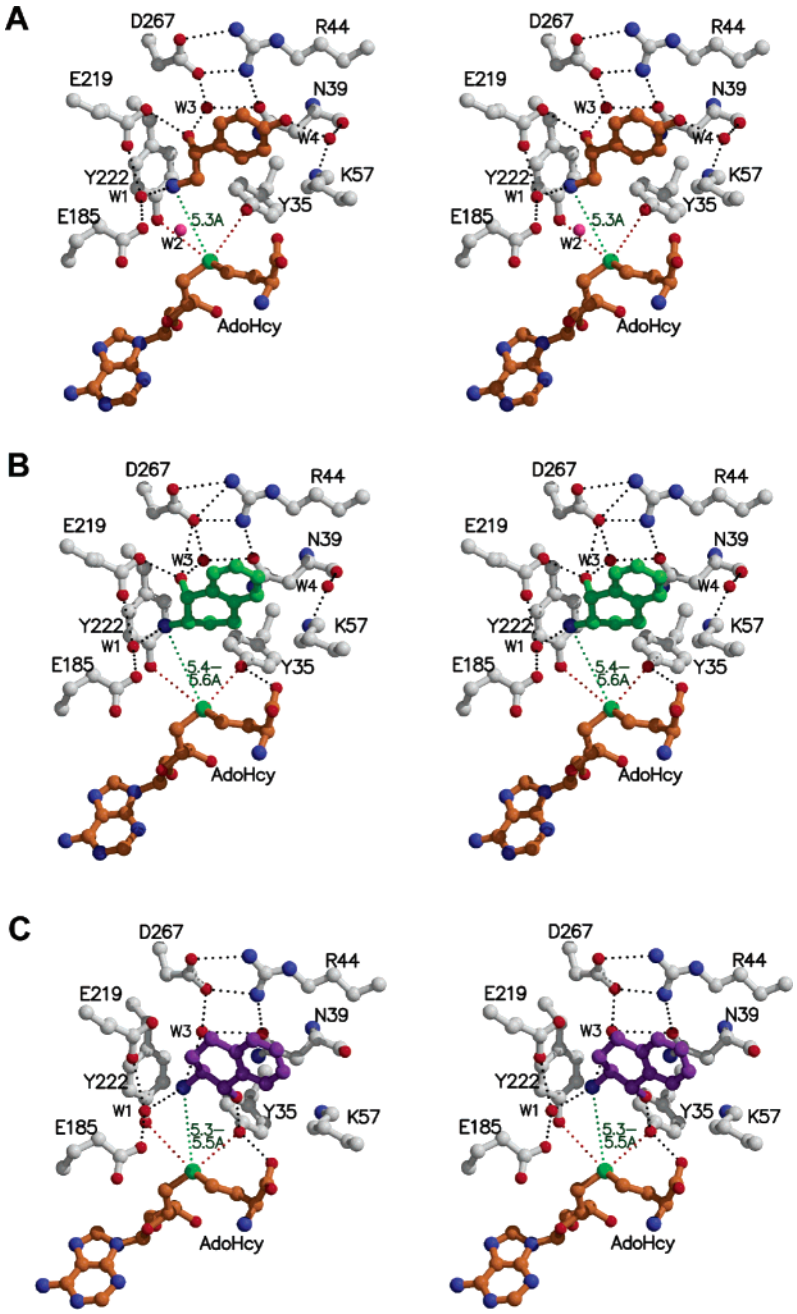

FIGURE 2: Stereoviews of (A) (*R*)-*p*-octopamine, (B) *cis*-(1*R*,2*S*)-AT, and (C) *trans*-(1*S*,2*S*)-AT bound in the active site of hPNMT. Hydrogen bonds are shown with black dotted lines. Interactions between the AdoHcy sulfur and tyrosine hydroxyls are shown with red dotted lines. The distances between the nitrogens of *p*-octopamine, *cis*-(1*R*,2*S*)-AT, or *trans*-(1*S*,2*S*)-AT and the sulfur of AdoHcy are shown with green dotted lines (the range indicates the measured values for both hPNMT complexes in the crystallographic asymmetric unit). The position of Wat2, described in the text, is shown in panel A.

positions of both A and B enzymes, the refined *B*-factors are 44.3 Å^2 (Wat1) and 50.2 Å^2 (Wat2) for hPNMT$_A$ and 53.9 Å^2 (Wat1) and 30.7 Å^2 (Wat2) for hPNMT$_B$. Electron density maps calculated from these structures reveal $2F_o - F_c$ density at 1σ for Wat1 in hPNMT$_B$ but negligible $2F_o - F_c$ density at 1σ for Wat2 in hPNMT$_A$. These results suggest that both water molecules may be present in both enzyme molecules in the asymmetric unit, but perhaps not at full occupancy. In any case, Wat2 may not be relevant to catalysis as it is likely to be displaced by AdoMet in the substrate complex and by the methylated product in the product complex.

cis-(1R,2S)-2-Aminotetralol (substrate). *cis*-(1*R*,2*S*)-AT is a conformationally restricted analogue of PEA; the freely rotatable β-hydroxyethylamine of PEA is constrained in *cis*-(1*R*,2*S*)-AT through cyclization. The (1*R*)-hydroxyl was thought to mimic the β-hydroxyl of PEA and the (2*S*)-amino group to mimic the extended conformation of the ethylamine (*17*). The crystal structure of hPNMT complexed with *cis*-(1*R*,2*S*)-AT confirms this, in that the hydroxyl group of *cis*-(1*R*,2*S*)-AT binds at the same position as the β-hydroxyl of *p*-octopamine and makes identical interactions with the enzyme. The amines of *cis*-(1*R*,2*S*)-AT and octopamine also bind to the enzyme in a similar manner (Figures 2A,B and 4B). The bound conformation of *cis*-(1*R*,2*S*)-AT is the low-energy half-chair conformation and is that predicted to interact with PNMT (*8*), with the hydroxyl group axial and the amine equatorial. The amine of *cis*-(1*R*,2*S*)-AT is a

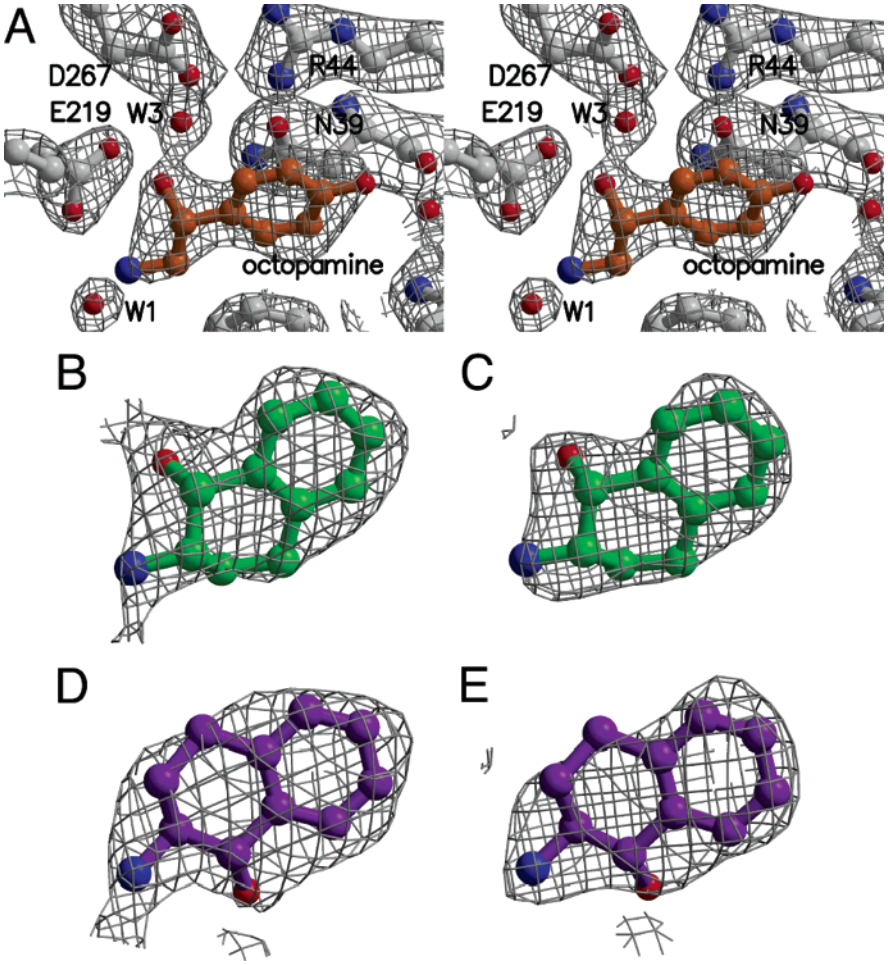

FIGURE 3: Simulated annealing $F_o - F_c$ omit electron density maps contoured at 4σ. (A) *p*-Octopamine showing interactions of the β-hydroxyl with Asp267 and Glu219. (B) *cis*-(1*R*,2*S*)-AT in the active site of $hPNMT_B$ (monomer B in the asymmetric unit). (C) *cis*-(1*R*,2*S*)-AT in the active site of $hPNMT_A$ (monomer A in the asymmetric unit). (D) *trans*-(1*S*,2*S*)-AT in the active site of $hPNMT_B$ (monomer B in the asymmetric unit). (E) *trans*-(1*S*,2*S*)-AT in the active site of $hPNMT_A$ (monomer A in the asymmetric unit).

similar distance from the sulfur of AdoHcy, and the angle between the C−N bond of the substrate and the sulfur of AdoHcy is also similar to those for octopamine (Table 4). The two water molecules identified near the amine of *p*-octopamine (described above) are also present in the *cis*-(1*R*,2*S*)-AT complex. In $hPNMT_A$, only Wat1 is modeled (*B*-factor = 33 Å^2), though $F_o - F_c$ density suggests that Wat2 may also be present at a lower occupancy. In $hPNMT_B$, both Wat1 and Wat2 are modeled, with *B*-factors of 35 and 29 Å^2, respectively.

trans-(1S,2S)-2-Aminotetralol (inhibitor). *trans*-(1*S*,2*S*)-AT is a stereoisomer of *cis*-(1*R*,2*S*)-AT, wherein the critical hydroxyl and amine groups are in a *trans* configuration with respect to each other. This isomer of AT is not methylated by PNMT, but it does bind to the enzyme and inhibits its activity (Table 1). The binding mode of the *trans*-(1*S*,2*S*)-AT identified from the crystal structure of the complex reveals that compared with *cis*-(1*R*,2*S*)-AT, the *trans* isomer is flipped by 180° through the plane of the aromatic ring (Figure 4D). A consequence of this flipped binding mode is that the hydroxyl of *trans*-(1*S*,2*S*)-AT does not interact with the acidic side chains of Asp267 and Glu219, but instead interacts with Tyr35 (Figure 2C). Surprisingly, the amine of the inhibitor is bound in a position similar to that observed for the two substrates, and Wat1 and Wat2 (described above for the substrate structures) are also present. It should be noted, however, that whereas the omit density for the hydroxyl group of *trans*-(1*S*,2*S*)-AT in $hPNMT_B$ was clearly defined at 4σ, the omit density for the hydroxyl of the ligand in $PNMT_A$ was poorly defined, suggesting that the interaction with Tyr35 is relatively weak (Figure 3C).

AdoMet Modeling. The finding that the amines of *trans*-(1*S*,2*S*)-AT (an inhibitor) and the two substrates *p*-octopamine and *cis*-(1*R*,2*S*)-AT were located in a similar position and almost equidistant from the sulfur of AdoHcy prompted us to investigate the catalytic arrangement further. A methyl group was modeled onto AdoHcy in the three crystal structures to generate a model of AdoMet. Distances and angles between the substrate acceptor amine and the AdoMet donor methyl were measured for all three structures (Table 4). The distances between the amine and the donor methyl for *p*-octopamine, *cis*-(1*R*,2*S*)-AT, and *trans*-(1*S*,2*S*)-AT were similar (3.7−3.9 Å). In contrast, the angles between the C−N bond and the donor methyl group are different for the substrates and the inhibitor. Thus, for *p*-octopamine and *cis*-(1*R*,2*S*)-AT, the angles are 89−93°, roughly tetrahedral. By comparison, the angle for nucleophilic attack by the amine of *trans*-(1*S*,2*S*)-AT is more than 30° larger (129−132°, Table 4).

Mutation of Key Residues. On the basis of the substrate-bound structures, it became apparent that Glu185 may play an important role in catalysis, since it makes water-mediated

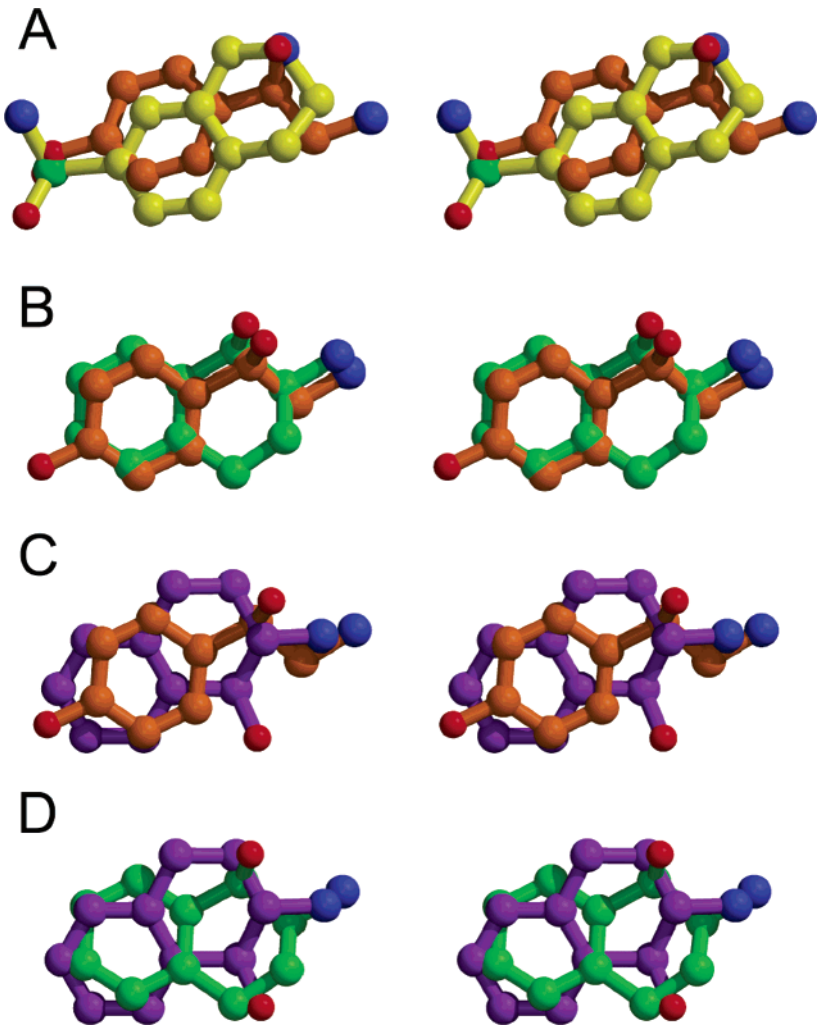

FIGURE 4: Overlays of molecules bound in the active site of hPNMT. (A) (*R*)-*p*-Octopamine (orange) and SK&F29661 (yellow) showing the position of the *β*-hydroxyl relative to the ring nitrogen of THIQ and the position of the *p*-hydroxyl of octopamine in relation to the 7-substituent of THIQs. (B) (*R*)-*p*-Octopamine (orange) and *cis*-(1*R*,2*S*)-AT (green). (C) (*R*)-*p*-Octopamine (orange) and *trans*-(1*S*,2*S*)-AT (purple). (D) *cis*-(1*R*,2*S*)-AT (green) and *trans*-(1*S*,2*S*)-AT (purple).

Table 3: Interactions of Enzyme with Bound Ligands[a]

	(*R*)-*p*-octopamine		*cis*-(1*R*,2*S*)-AT		*trans*-(1*S*,2*S*)-AT	
hPNMT atom	atom	distance (Å)	atom	distance (Å)	atom	distance (Å)
E219 O_{E1}	*β*-OH	2.9−3.0	1-OH	2.6−2.7	C3	2.9
D267 O_{D2}	*β*-OH	3.4−3.5	1-OH	3.3−3.4	C4	3.0−3.4
Wat3	*β*-OH	2.5−2.6	1-OH	2.5	C2	2.7−3.2
Wat1	NH_2	2.6[b]	2-NH_2	2.8−2.9	2-NH_2	3.1[b]
Wat2	NH_2	2.4[c]	2-NH_2	2.7[c]	2-NH_2	2.7[c]
Y222 C_{D2}	NH_2	3.4−3.5	2-NH_2	3.3−3.4	2-NH_2	3.8
Y35 OH					1-OH	2.6
M258 C_E	C3	3.5[b]	C6	3.5	C8	3.7
	C5	3.7[c]				
Wat4 (to K57)	*p*-OH	2.7−2.9				
F182 C_{D2}	C8	3.5−3.6	C2	3.4	C5	3.4[b]
F182 C_{E1}					C5	3.4[c]
V269 C_{G1}					C4	3.7

[a] Cutoffs are ≤3.5 Å for hydrogen bond or amino−aromatic and ≤3.8 Å for van der Waals interactions (only the closest interaction is listed). Atoms in octopamine and the two AT isomers are numbered according to Figure 1B. [b] $hPNMT_A$ only. [c] $hPNMT_B$ only.

interactions with the attacking amine. Also, on the basis of the interactions of the hydroxyl of *trans*-(1*S*,2*S*)-AT with Tyr35, it was of interest to examine the role of this residue. Therefore, the hPNMT variants Y35F, E185A, E185D, and E185Q were prepared as His-tagged derivatives. For comparative purposes, the E219Q variant was also prepared. In general, the yield of the purified protein for the mutants was similar to that of the wild-type enzyme, but the yield of the soluble protein for the E185A variant was greatly reduced. The reasons for this are unclear.

A comparison of the kinetic data for wild-type and variant hPNMTs [including the E219A, D267A, and D267N variants for which data have been reported previously (*19*)] is provided in Table 5. Both the E185A and E185Q mutants

Table 4: Distances and Angles for Substrate or Inhibitor Amines and Methyls and Sulfurs of AdoMet and AdoHcy, Respectively[a]

	N···S_D AdoHcy (Å)	N···C_E AdoMet (Å)	C−N···S_D AdoHcy (deg)	C−N···C_E AdoMet (deg)	Cγ−S_D···N AdoHcy (deg)	S_D−C_E···N AdoMet (deg)	C_{5*}−S_D···N AdoHcy (deg)
octopamine	5.3	3.7−3.8	90−93	89−92	93−94	141−144	97−98
cis-(1*R*,2*S*)-AT	5.4−5.6	3.7−3.9	91−93	91−93	99−100	151−154	100−101
trans-(1*S*,2*S*)-AT	5.3−5.5	3.7−3.8	129	129−132	93−96	153−157	109−113

[a] The range for each measurement indicates the values measured for each of the two complexes in the crystallographic asymmetric unit.

Table 5: Michaelis−Menten Data for hPNMT Variants[a,b]

hPNMT form	K_m(PEA)[c] (μM)	K_m(AdoMet) (μM)	k_{cat} (min^{-1})
wild type	99 ± 6	3.4 ± 0.2	2.8 ± 0.1
Y35F	1730 ± 15	45 ± 7	1.05 ± 0.11
E185A	102 ± 6	1.7 ± 0.1	0.17 ± 0.01
E185Q	101 ± 6	1.3 ± 0.1	0.01 ± 0.001
E185D	320 ± 32	14 ± 1	0.85 ± 0.04
E219A[b]	580 ± 76	7.1 ± 0.8	1.31 ± 0.11
E219Q	179 ± 17	6.7 ± 0.5	2.9 ± 0.1
D267A[b]	2050 ± 130	8.3 ± 0.7	0.13 ± 0.02
D267N[b]	1640 ± 70	7.1 ± 0.8	0.10 ± 0.01

[a] Kinetic data were obtained in 50 mM phosphate buffer (pH 8.0) at 30 °C. Each datum point is an average of at least three individual measurements. Values are reported as ±standard error of the mean (SEM). [b] Data from ref *19*. [c] PEA used in these assays was racemic.

were found to have values of K_m for PEA similar to that of wild-type hPNMT, suggesting that the mutations did not affect the binding mode of the substrate. Their K_m values for AdoMet were slightly lower than for the wild type. The E185D variant had moderately increased K_m values for both PEA and AdoMet. Most importantly, the k_{cat} values for E185D, E185A, and E185Q were reduced by 3-, 15-, and ~300-fold, respectively, suggesting that this residue may play an important, albeit not critical, role in catalysis. Intriguingly, the most dramatic effect on catalysis was that caused by mutation of Glu185 to the nonacidic Gln. By comparison, the E219Q mutant had no effect on the catalytic rate.

Replacement of Tyr35 with phenylalanine substantially reduced the level of binding of PEA and AdoMet. The effect of this mutation on AdoMet binding is perhaps not surprising as the Tyr35 hydroxyl interacts with a carboxylate oxygen of the amino acid portion of AdoHcy and, presumably, of AdoMet (*16*). However, it is not clear why the binding of PEA was affected by this mutation as there are no obvious interactions between PEA and Tyr35. The reduced binding affinity of PEA may, however, simply be a consequence of the weaker binding of AdoMet; the enzyme is likely to undergo a conformational change to enable access to the active site for both cofactor and substrate (or inhibitor) (*17*), and binding of the large AdoMet cofactor may help induce these changes. Mutation of Tyr35, located close to an unusual type VIa (*cis*-Pro) β-turn (Pro42-Pro43) suggested as a hinge point for conformational change (*17*), may affect the energetics of such conformational changes and thus affect PEA binding. More surprising was the fact that the catalytic rate was not greatly affected by the Y35F mutation, indicating that the hydroxyl of Tyr35 is not significantly involved in catalysis.

DISCUSSION

The crystal structures of hPNMT complexed with substrates *p*-octopamine and *cis*-(1*R*,2*S*)-AT show that the constrained conformation of the latter does represent the bound conformation of the flexible substrates. Kinetic analysis of *cis*-(1*R*,2*S*)-AT shows that it binds 1 order of magnitude more tightly to hPNMT than its flexible counterpart PEA, and that whereas the k_{cat} value is lower for *cis*-(1*R*,2*S*)-AT, methyl transfer (k_{cat}/K_m) for this substrate is slightly more efficient than for PEA (Table 1). The crystal structures show that the amine and hydroxyl groups of the semirigid *cis*-(1*R*,2*S*)-AT substrate form the same interactions as those of the flexible substrate, indicating that the semirigid analogue gains an entropic advantage over PEA for binding to PNMT.

Role of the β-Hydroxyl of PNMT Substrates. The crystal structures also confirm that the amines in THIQ inhibitors of PNMT mimic the binding of the β-hydroxyl group of the substrate. The β-hydroxyl is thought to be critical for substrate activity; no substrate activity was found for dopamine (*5*) (the compound corresponding to norepinephrine without the β-hydroxyl), and instead, it inhibits the enzyme (*5*). However, the presence of a β-hydroxyl group is not an absolute requirement, since conformationally defined rigid analogues lacking a hydroxyl group are substrates (*12*, *13*). Furthermore, it is possible to replace the β-hydroxyl with other hydrogen bond donors and still maintain substrate activity; thus, the diamino (β-amino) compound phenylethylenediamine is a substrate of the rabbit enzyme (*5*). Nonetheless, it is clear that in physiological substrates of PNMT, the β-hydroxyl group is critical for activity.

The β-hydroxyl makes several strong interactions with hPNMT, and these interactions may help to select the conformation of the flexible ethanolamine side chain that correctly positions the amine for nucleophilic attack. Furthermore, in the absence of the β-hydroxyl, the amine of flexible ethylamine substrates has the potential to interact with either Glu219 or Asp267 rather than with Glu185. This could explain why dopamine and phenylethylamine, which lack the β-hydroxyl group, are inhibitors rather than substrates of PNMT. The strong water-mediated interaction formed with Asp267 by the β-hydroxyl may also act to anchor the substrate in the active site so that it does not slide away from the methyl donor during catalysis. Noteworthy in this context is the fact that there are very few other hydrogen bond interactions with the substrate that could keep it locked in place in the large binding site of the enzyme. The kinetic data for the D267A and D267N variants of hPNMT support the notion that this residue is important for orienting and anchoring the substrate (*19*). Substrates with a flexible ethanolamine side chain exhibit lower values of k_{cat} with Asp267 variants compared to that with the *wt* enzyme (Table 5 and ref *19*), but the value of k_{cat} is relatively unchanged for a rigid analogue substrate (*19*). The E219A

variant shows a much smaller effect than the Asp267 variants on both K_m and k_{cat}, suggesting that this residue plays a lesser role, if any, in substrate orientation and catalysis. The reasons for this are not clear, though the electron density and refined structure support the kinetic data in that stronger (shorter) bonds are formed from the substrate (via a water) to Asp267 compared with Glu219. Interestingly, the k_{cat} values for the alanine and asparagine variants of Asp267 are both 20−30-fold lower than the wild-type value, suggesting that an ionized carboxylate is important, while for both the alanine and glutamine variants of Glu219 the effect on k_{cat} is negligible, suggesting that its ionization state is less important.

Proposal for the Catalytic Mechanism of PNMT. Methyltransferases are thought to catalyze direct transfer of the methyl group from AdoMet to the substrate via an S_N2 mechanism (*30*). The crystal structures of glycine *N*-methyltransferase (GNMT) and guanidinoacetate *N*-methyltransferase (GAMT) have been used to model the catalytic substrate−cofactor complexes and to propose catalytic mechanisms for *N*-methyl transfer by these small molecule *N*-methyltransferases (*31*, *32*). In GAMT, acidic residues are proposed to deprotonate the acceptor amine so that it forms a sufficiently strong nucleophile to attack the methyl group of the cofactor, AdoMet (*31*). In GNMT, glycine is held in position by hydrogen bonds that orient the lone pair orbital of the glycine nitrogen toward the methyl group of AdoMet. Thus, GNMT appears to catalyze methyl transfer via "proximity and orientation effects" (*31*). There are no acidic residues close to the amine, and the substrate is proposed to be bound in the neutral form (*31*). The lone pair of the neutral amine acts as the nucleophile for S_N2 attack on the methyl group of AdoMet. For GAMT, there are several acidic residues in the vicinity of the amine, and the amine is thought to be protonated when initially bound so that deprotonation would need to occur prior to nucleophilic attack. In both enzymes, thermal motion is thought to lead to collision of the lone pair of the substrate amine and the methyl group of the cofactor so that S_N2 transfer of the methyl group to the acceptor amine takes place (*32*).

The hPNMT structural and kinetic data presented here suggest that this enzyme also catalyzes methyl transfer through proximity and orientation effects. Thus, a major role of the enzyme is to position and anchor correctly the two substrates, the methyl donor AdoMet and the acceptor substrate. Asp267 probably plays a role in anchoring the β-hydroxyl and Glu185 in anchoring the amine. The geometries of the acceptor amines of the substrates for both PNMT and GNMT (glycine modeled in GNMT and octopamine or *cis*-AT in hPNMT) are similar and indicate that the reaction for PNMT is an S_N2 nucleophilic attack by the substrate amine on the activated methyl group of the cofactor (tetrahedral geometry of the amine lone pair with C_E, collinearity of the amine with the S_D-C_E bond vector) (*19*, *33*).

In GAMT, deprotonation is thought to occur through a direct interaction between the substrate amine and the side chain of an aspartic acid residue (*31*). In hPNMT, the X-ray structures suggest that deprotonation is most likely to occur through the water-mediated interactions with Glu185 or Glu219 (Figure 5). When Glu185 is replaced with glutamine, the catalytic rate drops 300-fold; the E185D variant exhibited only a 3-fold decrease. This suggests that it is crucial for the carboxylate to be ionized, and supports the notion that Glu185 assists in deprotonation of the amine. Changing the carboxylate to an amide probably disrupts the hydrogen bond network among the substrate and Glu185, Wat1, and Glu219 (Figures 2 and 5); the Glu185 side chain is positioned by interactions with two hydrogen bond donors (Figure 5) which would not interact favorably with a glutamine side chain.

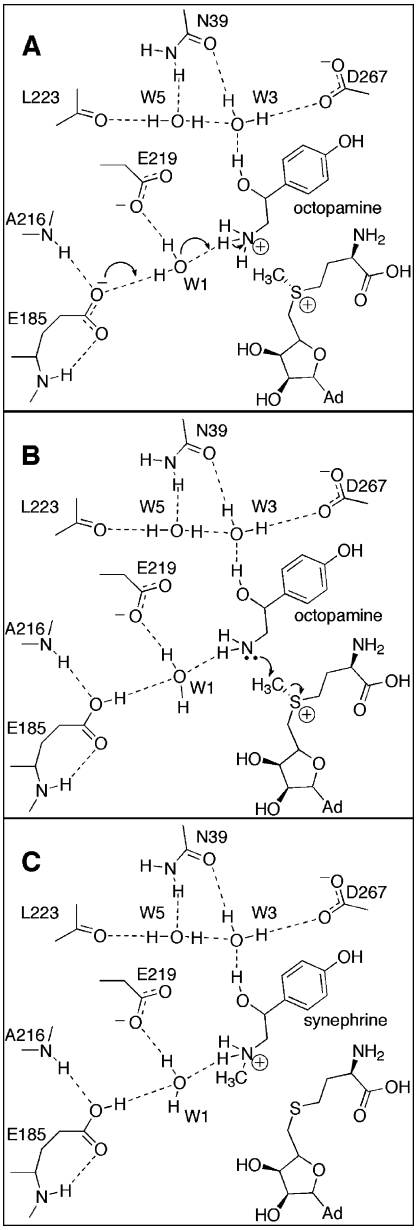

FIGURE 5: Proposed reaction mechanism for methyl transfer by hPNMT. (A) Deprotonation. The amine is likely to be protonated when bound in the active site, due to the presence of nearby acidic residues. Deprotonation of the amine is required prior to the S_N2 reaction. In the proposed mechanism, a proton is abstracted from the octopamine amine by Glu185 via a bridging water. Hydrogen bonding distances between atoms are listed in Table 3. (B) Nucleophilic attack. Thermal motion of the enzyme induces collision of the amine lone pair with the AdoMet methyl group, allowing methyl transfer to proceed via an S_N2 mechanism. (C) Products of the reaction, methylated octopamine and AdoHcy, are bound in the active site. Ad refers to the adenine ring of AdoMet and AdoHcy.

Disruption of the network in E185Q could conceivably result in repositioning of the water such that it is unable to abstract a proton from the substrate. By comparison, an E219Q mutation would not disrupt the network in the same way since the side chain interacts with atoms that can act as hydrogen bond donors or acceptors. However, and surprisingly, the E185A variant barely exhibited a 10-fold decrease in k_{cat} compared with that of the wild type. This could be either due to an effect on active site hydrophobicity such that the substrate amine is not protonated when bound or because the E185A mutant allows the attacking water to attain a reasonable, but certainly not optimal, position for the reaction to proceed. The overall lack of an effect of the substitutions of Glu219 indicates that Glu185 plays a more significant role than Glu219 in catalysis. However, a full explanation of the mutagenesis results and a further indication of the role of Glu185 must await the determination of the structures of E185Q and E185A mutant hPNMTs in complex with substrate.

The structural evidence indicates that the acceptor amines interact directly with the protein in the N-methylation of glycine by GNMT (*32*) and guanidinoacetate by GAMT (*31*), rather than through water-mediated interactions shown by hPNMT. Another difference between hPNMT and these two enzymes is the distance between the acceptor amine and the sulfur of AdoHcy (or methyl of modeled AdoMet). For GAMT and GNMT, the amine−sulfur distance is ~4 Å, whereas the same distance is ~1.5 Å longer in hPNMT (5.3−5.6 Å). The amine and sulfur are oriented correctly for an S_N2 reaction, but they are further apart in hPNMT than in the other two enzymes. This suggests that PNMT makes somewhat larger movements to bring the two substrates together during catalysis.

PNMT Substrate versus Inhibitor. The pair of structures of the enzyme complexed with the *cis* and *trans* isomers of AT might have been expected to reveal different bound positions of the amine so that the *trans* isomer amine would be positioned farther from the cofactor than the *cis* isomer amine, thus explaining its inhibitory rather than substrate activity. However, the distances between the sulfur of AdoHcy (or the modeled methyl group of AdoMet) and the acceptor amines of all three ligands are similar and do not allow discrimination between substrates and inhibitors. However, the angles of approach between the amine and the AdoHcy sulfur or AdoMet methyl do differ considerably between substrate (~90°) and inhibitor (130°) and may offer a possible means of discrimination by the enzyme.

Other explanations for the differing activities of the two AT isomers were suggested from a comparative structural analysis. One difference we observed was that *trans*-(1*S*,2*S*)-AT, unlike the substrates *cis*-(1*R*,2*S*)-AT and *p*-octopamine, interacts through hydrogen bonds with Tyr35. This interaction suggested the possibility that Tyr35 may play a role in catalysis, perhaps like that described for a tyrosine in GNMT (*32*), which is thought to stabilize the transition state by making a charge−dipole interaction with the positively charged sulfur of AdoMet during catalysis. If Tyr35 played a similar role in PNMT catalysis, the interaction with *trans*-(1*S*,2*S*)-AT might very well interfere with the process, giving rise to inhibition rather than catalysis. However, the kinetic analysis of Y35F hPNMT showed that Tyr35 is not essential for catalysis, effectively ruling out this possibility.

A second, and perhaps more plausible, explanation for why PNMT does not utilize *trans*-(1*S*,2*S*)-AT as a substrate is the strength and positioning of anchor points in the binding site. We described above how the β-hydroxyl of *p*-octopamine and the equivalent hydroxyl of *cis*-(1*R*,2*S*)-AT form strong interactions especially with Asp267, which may serve to anchor the substrate during catalysis. By comparison, the hydroxyl group of *trans*-(1*S*,2*S*)-AT interacts with Tyr35 only, and the poor quality of the electron density for this group in comparison to that for the water-bridged Asp267 interaction suggests a relatively weak interaction. The similar positioning of the amines but differing positions and strengths of the hydroxyl interactions of *cis*-(1*R*,2*S*)-AT and *trans*-(1*S*,2*S*)-AT suggests that *trans*-(1*S*,2*S*)-AT may not be utilized as a substrate because it lacks the correct or sufficient anchoring. In this context, it should be noted that rigid analogues exist that are PNMT substrates but that lack hydroxyls, for example, *anti*-9-aminobenzonorbornene (Figure 1). This compound therefore does not have the hydroxyl "anchor" that we propose is required for substrate activity. However, our preliminary modeling of this compound in the active site of the enzyme suggests that the bridging methylenes would occupy a position similar to that of the β-hydroxyl of octopamine, and this could provide a steric (rather than a hydrogen bond) anchoring constraint.

ACKNOWLEDGMENT

We thank John de Jersey for helpful discussions and Kevin R. Criscione for his assistance with the manuscript.

REFERENCES

1. Minson, J., Llewellyn-Smith, I., Neville, A., Somogyi, P., and Chalmers, J. (1990) Quantitative analysis of spinally projecting adrenaline-synthesising neurons of C1, C2 and C3 groups in rat medulla oblongata, *J. Auton. Nerv. Syst. 30*, 209−20.
2. Kovachich, G. B., and Mishra, O. P. (1983) Inhibition of norepinephrine autoxidation by a rat brain cortical factor, *Neurosci. Lett. 37*, 63−8.
3. Axelrod, J. (1962) Purification and properties of phenylethanolamine-*N*-methyl transferase, *J. Biol. Chem. 237*, 1657−60.
4. Fuller, R. W., and Hunt, J. M. (1965) Substrate specificity of phenethanolamine *N*-methyl transferase, *Biochem. Pharmacol. 14*, 1896−7.
5. Fuller, R. W., Warren, B. J., and Molloy, B. B. (1970) Substrate specificity of phenethanolamine *N*-methyltransferase from rabbit adrenal, *Biochim. Biophys. Acta 222*, 210−2.
6. Fuller, R. W., Hemrick-Luecke, S. K., and Midgley, J. M. (1981) Comparison of o-octopamine and related phenylethanolamines as substrates for norepinephrine *N*-methyltransferase, *Res. Commun. Chem. Pathol. Pharmacol. 33*, 207−13.
7. Krakoff, L. R., and Axelrod, J. (1967) Inhibition of phenylethanolamine-*N*-methyl transferase, *Biochem. Pharmacol. 16*, 1384−6.
8. Grunewald, G. L., Ye, Q., Kieffer, L., and Monn, J. A. (1988) Conformational requirements of substrates for activity with phenylethanolamine *N*-methyltransferase, *J. Med. Chem. 31*, 169−71.
9. Grunewald, G. L., and Ye, Q. (1988) Stereochemical aspects of phenylethanolamine analogues as substrates of phenylethanolamine *N*-methyltransferase, *J. Med. Chem. 31*, 1984−6.
10. Grunewald, G. L., Sall, D. J., and Monn, J. A. (1988) Conformational and steric aspects of the inhibition of phenylethanolamine *N*-methyltransferase by benzylamines, *J. Med. Chem. 31*, 433−44.
11. Ye, Q., and Grunewald, G. L. (1989) Conformationally restricted and conformationally defined tyramine analogues as inhibitors of phenylethanolamine *N*-methyltransferase, *J. Med. Chem. 32*, 478−86.

12. Rafferty, M. F., and Grunewald, G. L. (1982) The remarkable substrate activity for phenylethanolamine *N*-methyltransferase of some conformationally defined phenylethylamines lacking a side-chain hydroxyl group. Conformationally defined adrenergic agents. 6, *Mol. Pharmacol. 22*, 127−32.
13. Grunewald, G. L., Markovich, K. M., and Sall, D. J. (1987) Binding orientation of amphetamine and norfenfluramine analogues in the benzonorbornene and benzobicyclo[3.2.1]octane ring systems at the active site of phenylethanolamine *N*-methyltransferase (PNMT), *J. Med. Chem. 30*, 2191−208.
14. Grunewald, G. L., Pleiss, M. A., and Rafferty, M. F. (1982) Conformational preferences of dopamine analogues for inhibition of norepinephrine *N*-methyltransferase. Conformationally defined adrenergic agents, *Life Sci. 31*, 993−1000.
15. Grunewald, G. L., Arrington, H. S., Bartlett, W. J., Reitz, T. J., and Sall, D. J. (1986) Binding requirements of phenolic phenylethylamines in the benzonorbornene skeleton at the active site of phenylethanolamine *N*-methyltransferase, *J. Med. Chem. 29*, 1972−82.
16. Martin, J. L., Begun, J., McLeish, M. J., Caine, J. M., and Grunewald, G. L. (2001) Getting the adrenaline going: Crystal structure of the adrenaline-synthesizing enzyme PNMT, *Structure 9*, 977−85.
17. McMillan, F. M., Archbold, J., McLeish, M. J., Caine, J. M., Criscione, K. R., Grunewald, G. L., and Martin, J. L. (2004) Molecular recognition of sub-micromolar inhibitors by the epinephrine-synthesizing enzyme phenylethanolamine *N*-methyltransferase, *J. Med. Chem. 47*, 37−44.
18. Grunewald, G. L., Skærbæk, N., and Monn, J. A. (1993) in *Trends in QSAR and Molecular Modelling '92* (Wermuth, C. G., Ed.) pp 513−6, ESCOM Science Publishers B. V., Leiden, The Netherlands.
19. Wu, Q., Gee, C. L., Lin, F., Tyndall, J. D., Martin, J. L., Grunewald, G. L., and McLeish, M. J. (2005) Structural, mutagenic and kinetic analysis of the binding of substrates and inhibitors of human phenylethanolamine *N*-methyltransferase, *J. Med. Chem. 48*, 7243−7252.
20. Romero, F. A., Vodonick, S. M., Criscione, K. R., McLeish, M. J., and Grunewald, G. L. (2004) Inhibitors of phenylethanolamine *N*-methyltransferase that are predicted to penetrate the blood-brain barrier: Design, synthesis and evaluation of 3-fluoromethyl-7-(*N*-substituted aminosulfonyl)-1,2,3,4-tetrahydroisoquinolines that possess low affinity toward the α_2-adrenoreceptor, *J. Med. Chem. 47*, 4483−93.
21. Gee, C. L., Nourse, A., Hsin, M., Wu, Q., Tyndall, J. D., Grunewald, G. L., McLeish, M. J., and Martin, J. L. (2005) Disulfide-linked dimers of human PNMT are catalytically active, *Biochim. Biophys. Acta 1750*, 82−92.
22. Brünger, A. T., Adams, P. D., Clore, G. M., Delano, W. L., Gros, P., Grosse-Kunstleve, R. W., Jiang, J. S., Kuszewski, J., Nilges, N., Pannu, N. S., Read, R. J., Rice, L. M., Simonson, T., and Warren, G. L. (1998) Crystallography and NMR system (CNS): A New Software System for Macromolecular Structure Determination, *Acta Crystallogr. D54*, 905−21.
23. Jones, T. A., Zou, J. Y., Cowan, S. W., and Kjeldgaard, M. (1991) Improved methods for building protein models in electron density maps and the location of errors in these models, *Acta Crystallogr. A47*, 110−9.
24. Murshudov, G. N., Vagin, A. A., and Dodson, E. J. (1997) Refinement of Macromolecular Structures by the Maximum-Likelihood Method, *Acta Crystallogr. D53*, 240−55.
25. Schuettelkopf, A. W., and van Aalten, D. M. F. (2004) PRODRG: A tool for high-throughput crystallography of protein−ligand complexes, *Acta Crystallogr. D60*, 1355−63.
26. Kleywegt, G. J., and Jones, T. A. (1998) Databases in protein crystallography, *Acta Crystallogr. D54*, 1119−31.
27. Brünger, A. T. (1992) Free *R* value: A novel statistical quantity for assessing the accuracy of crystal structures, *Nature 355*, 472−5.
28. Segel, I. (1975) *Enzyme Kinetics*, Wiley & Sons, New York.
29. Cleland, W. W. (2000) Low-barrier hydrogen bonds and enzymatic catalysis, *Arch. Biochem. Biophys. 382*, 1−5.
30. Schubert, H. L., Blumenthal, R. M., and Cheng, X. (2003) Many paths to methyltransfer: A chronicle of convergence, *Trends Biochem. Sci. 28*, 329−35.
31. Komoto, J., Yamada, T., Takata, Y., Konishi, K., Ogawa, H., Gomi, T., Fujioka, M., and Takusagawa, F. (2004) Catalytic mechanism of guanidinoacetate methyltransferase: Crystal structures of guanidinoacetate methyltransferase ternary complexes, *Biochemistry 43*, 14385−94.
32. Takata, Y., Huang, Y., Komoto, J., Yamada, T., Konishi, K., Ogawa, H., Gomi, T., Fujioka, M., and Takusagawa, F. (2003) Catalytic mechanism of glycine *N*-methyltransferase, *Biochemistry 42*, 8394−402.
33. Dafforn, G. A., and Koshland, D. E., Jr. (1971) The sensitivity of intramolecular reactions to the orientation of the reacting atoms, *Bioorg. Chem. 1*, 129−39.

BI051636B